"Modal Analysis of Turbine Blades Considering Edge Hard Body Impact"

[1]Tejesh S, [2]Amith Kumar S N, [3]Chandan R, [4]Dr. Vinod K L

[1234]Assistant Professor

[1234]Department of Mechanical Engineering

[1234]Dr. Ambedkar Institute of Technology, Bengaluru, India

DOI: https://doi.org/10.51584/IJRIAS.2025.100600125

Received: 26 June 2025; Accepted: 03 July 2025; Published: 19 July 2025

ABSTRACT

Since the beginning of the Turbo machinery, modal analysis has been crucial to the designers and operators. Low-cycle fatigue (LCF), high-cycle fatigue (HCF), environmental attack, creep, oxidation, erosion, and embrittlement are the usual causes of blade failure. The eigen value extraction for the flexural and torsional modes is obtained by modeling and analyzing the turbine blade using the finite element approach in this work. A circular crack along the blade's leading edge is used to imitate damage from foreign objects. The increase in the structure's bending stiffness was discovered to be caused by the stretching brought on by the centrifugal inertia force as a result of the blades' rotation. This led to the highest operational Von-mises stresses; the goal is to give designers knowledge and insight to extend the lifespan and efficiency of gas turbines.

Key words: Eigen value, low cycle fatigue, high cycle fatigue, turbine blade.

INTRODUCTION

When a periodic force operates at a frequency that matches the inherent frequency of a blade, resonance occurs, which is a significant failure mechanism. If the damping is

When the periodic input energy is not adequately absorbed, the amplitude and stresses increase until overstress or fatigue fracture propagation cause failure. The surface is covered in a complicated and asymmetrical pattern of small indentations, including strikes from leading edges. Damage from foreign objects frequently takes the shape of a notch or other geometric discontinuity. However, the use of basic notch analyses is prohibited by the existence of residual stress and sub-structural damage in areas next to the notch. The stress concentration impact of the notch's geometry is estimated using FE analysis. For FEM research, the compressor aerofoil blade is idealized into a straightforward rectangular cantilever plate.

Assuming that the aerofoil section is a planar rectangular plate, the problem is simplified to a simplex problem. The absence of the aerofoil section makes it very easy to analyze and determine the stress concentration impact of the geometrical notch that was formed. Different notches are created by altering the notch's dimensions, such as its depth, radius, and placement on the rectangular plate's trailing edge, in order to examine the stress concentration effect of foreign object damage (FOD).

Using a high-speed grinding wheel, foreign object-damaged compressor blades with nicks, dents, and cracks can be ground into the smooth curved cutouts to lessen stress concentration and intensification. The designer must predict the size and shape of the cut-out that will be made on the aerofoil in order to generate the known SCF, depending on the type and level of damage. The finite element analysis is performed on a rectangular cantilever plate for which literature is available. Using the estimated values of SCF for various cut geometries using FEM, a modal analysis has been performed to evaluate the variation of frequencies for various cut-out geometries with known values of SCF to confirm the accuracy of the solution.

ISSN No. 2454-6194 | DOI: 10.51584/IJRIAS |Volume X Issue VI June 2025

The subject is further expanded to include an idealized problem of a rectangular cantilever plate with and without notches in both static and rotating settings.

Figure 1: Impacts with a round shape

Theoretical Foundation

Every component of the beam oscillates up and down at the same frequency in a normal mode. As can be seen below, the oscillation amplitude changes throughout the beam for each of the first four normal modes (Y(x) is exaggerated). The beam's shape at the oscillation's extreme, when every point on the beam is instantly at rest, is depicted in figure 2 by Y(x). At the same moment, every point experiences zero displacement. The horizontal scale is represented as a fraction of the beam's total length, □, and the vertical displacement with respect to the fixed end is denoted by Y(x). Formally speaking, a cantilever is a beam that is limited in its Y(x) = 0 and

$$\frac{dY(x)}{dx} = 0$$ at x = 0 and the other end free.

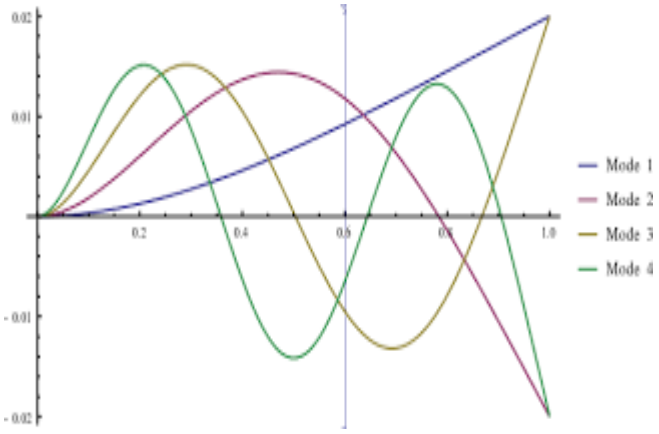

Figure 2: Shape of Modes

The parameters that determine the shape, Y(x), are as follows:

□ The length of the beam [m]

A The cross-sectional area of the beam [m^2]

ρ The mass density of the material [kg m^{-3}]

E Young's modulus for the material [kg m^{-1} s^{-2}]

ISSN No. 2454-6194 | DOI: 10.51584/IJRIAS |Volume X Issue VI June 2025

I A geometrical property called the second moment of area of the cross-section. For a rectangular cross-section of width, w, and thickness, d, this is given by $I = \frac{wd^3}{12}$

The theoretical expression for the displacement of the free end of a static cantilever is: $Y(\ell) = \frac{\rho A g}{8EI}\ell^4$

[g is the acceleration due to gravity]

If, in addition, a load of mass m is suspended from the free end the displacement is increased to $Y(\ell) = \frac{\rho A g}{8EI}\ell^4 + \frac{mg}{3EI}\ell^3$ Measurements on the static beam can therefore give information about groups of parameters, such as $\frac{\rho A}{EI}$ or EI. We shall see that these parameters are relevant to its dynamic behaviour.

In mode 1, all parts of the beam move, except the fixed end. In mode 2 there is a stationary point, or *node*, away from the end (at x/□ = 0.784). In mode 3 there are two nodes, and so on.

For Flexural Modes

The Natural frequency of flexural modes

$\omega_n = \beta^2_n \sqrt{(EI / \rho L)}$

The vibration of beam with constant mass and stiffness is given by

$$EI\frac{\partial^4 \bar{y}}{\partial \bar{x}^4} + m\frac{\partial^2 \bar{y}}{\partial \bar{t}^2} = \bar{f}(\bar{x}, \bar{t}), \qquad 0 < x < l,$$

Substituting the above expression into the homogeneous form

where β_j is the jth positive root of the equation

$$Y^{(4)}T + Y\ddot{T} = 0,$$

$$\frac{Y^{(4)}}{Y} = -\frac{\ddot{T}}{T} = \beta^4, \qquad \cos\beta_j \cosh\beta_j = -1, \quad \text{and} \quad \alpha_j = \frac{\cosh\beta_j + \cos\beta_j}{\sinh\beta_j + \sin\beta_j}$$

For Torsional Modes

The angular frequencies, ω_n, of the normal modes, are given by

$$\omega_n = 2\pi\upsilon_n = \frac{\theta_n^2}{\ell^2}\sqrt{\frac{EI}{\rho A}} = \theta_n^2\sqrt{\frac{EI}{\rho A \ell^4}}$$

θ_n is a number. The general solution Y(x) of the form

$$Y_n(x) = \cosh\left(\theta_n \frac{x}{\ell}\right) - \cos\left(\theta_n \frac{x}{\ell}\right) - \sigma_n\left[\sinh\left(\theta_n \frac{x}{\ell}\right) - \sin\left(\theta_n \frac{x}{\ell}\right)\right]$$

In which the θ_n are the solutions of cosh (θ_n) cos (θ_n) = -1

ISSN No. 2454-6194 | DOI: 10.51584/IJRIAS |Volume X Issue VI June 2025

$$\sigma_n = \frac{\sinh(\theta_n) - \sin(\theta_n)}{\cosh(\theta_n) + \cos(\theta_n)}$$

And the θ_n are given by

Finite Element Formulation

ANSYS macros, which must be typed in the ANSYS command prompt box, are used to model and mesh the plate shape depicted in the figure. Using the RECTNG or BLC4/BLC5 macro commands under the /PREP7 pre-processor, the plate's dimensions—length L=200mm, width D=50mm, and thickness t=5mm—were modeled by providing the plate's equal dimensions in the corresponding working plane coordinates.

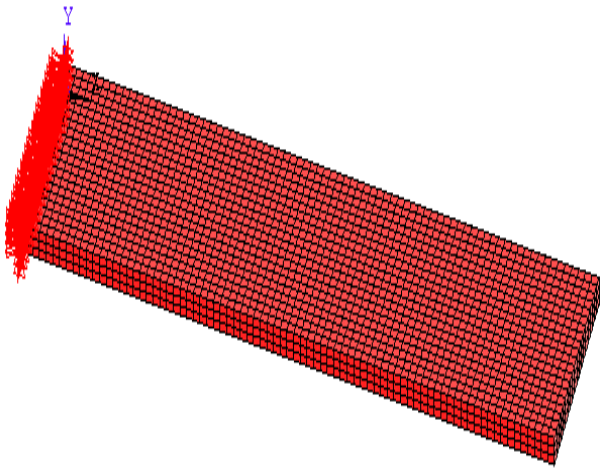

Figure 3: Finite Element model of a Rectangular Blade

The material taken for the plate is steel, have properties

Young's Modulus = 2.1e5 MPa.

Density = 7850 Kg/m^3

Poisson's ratio = 0.3

The material is assumed to be in linear isotropic elastic condition.

The blade is assumed to be rotating at a speed of 15000 rpm and the angular velocity of the blade is calculated from the available data as

$$\omega = \frac{2\pi N}{60} = \frac{2\pi * 15000}{60} = 1570796 \text{ rad/sec}$$

The model is marked into areas by lines for map meshing around the notch geometry and the macros used issued for material properties are entered by the commands MP, DENS-for density, MP-EX for Young's modulus and MP-PRXY-for Poisson's ratio in this context. The element type for this model taken is PLANE42 and SOLID45and written in macro commands by using ET-for element type. The model is fine meshed and coarse meshed the LESIZE-line element size and divisions and AMESH-area mesh as shown in figure .after meshing the plane 42 element, then the plane 42 element type is extruded to SOLID45 by using the EXT command. After extruding the PLANE42 elements are deleted and the nodes along z=0 are selected. The model is arrested in X, Y and Z direction by selecting the nodes to be fixed with D. The node selection is made by the NSEL with S or R command.

The solution phase begins with /SOLU command and the modal analysis type is switch on by writing ANTYPE, 1. The problem is solved by using the SOLVE macro command. The Post processing of results can be carried by the sequence of /POST1. The model consists of 4800 SOLID45 elements.

ISSN No. 2454-6194 | DOI: 10.51584/IJRIAS |Volume X Issue VI June 2025

RESULTS AND DISCUSSIONS

To determine the natural frequencies and dynamic responses of the beam, a free and forced vibration analysis of a rectangular cantilever beam was conducted for a range of notch values. Figure 4 displays the average natural frequency for First Flexural (1F) and First Torsion (1T) for notch dimension h=20mm. The notch radius increases from 1 to 10mm in increments of 1mm, and the corresponding values are 371.928 Hz and 892.041 Hz. A drop in the 1 F frequency is noted. The leading edge with the notch is where the centrifugal force is applied.

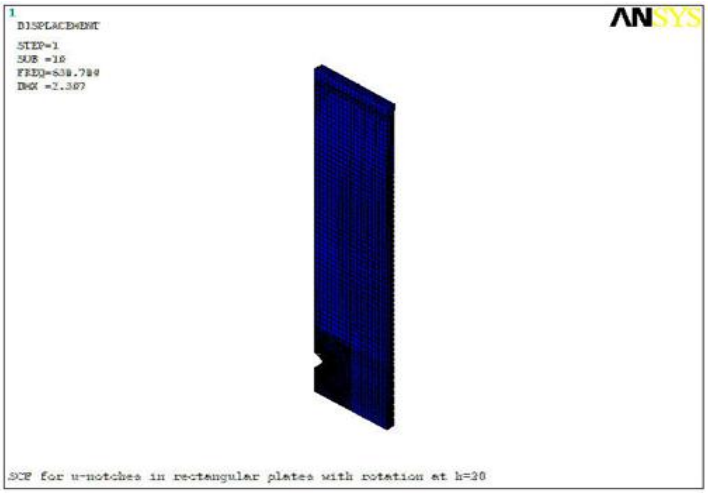

Figure 4: FEA model of rectangular blade with semicircular notch at h = 20mm

The angular velocity, which is computed with a constant engine speed of 15,000 rpm, yields the centrifugal force. With several location heights of 20 mm, 80 mm, 100 mm, 120 mm, and 150 mm from the blade's root to tip along the leading edge, the notch radius is adjusted in increments of 2 mm from 2 mm to 10 mm. It is noted that frequency falls from the blade's root to its tip for a notch radius of 2 mm and at the locations specified. As seen in figure 5, the percentage drop in 1F frequency for a 2 mm notch radius from the starting height of 20 mm to the finished height of 150 mm is 0.145%.

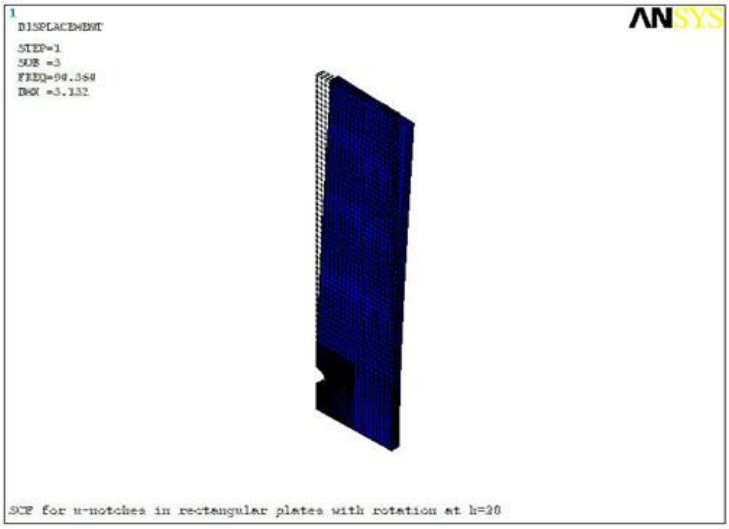

Figure 5: 1F mode of rectangular blade with semicircular notch at h = 20mm

Frequency rises from the blade's root to its tip for additional notch radius expansion in increments of 2 mm for the specified locations. From the starting height of 20 mm to the finished height of 150 mm, there is a 0.02% increase in 1F frequency for a 4 mm notch radius. According to Graph, the percentage increase in frequency for 1F frequency with an additional 6 mm notch radius increase and the height given is 0.3%.

ISSN No. 2454-6194 | DOI: 10.51584/IJRIAS |Volume X Issue VI June 2025

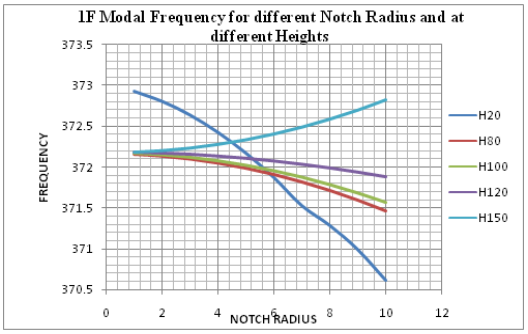

Graph 1. 1F Modal Frequency for different Notch Radius and at different Heights

As illustrated in figure 6, the first torsional frequency (1T) with a notch positioned 20 mm from the root and with a notch radius of 1 mm is 906.605 Hz. There is a little drop in the 1T frequency as the notch radius is extended from 1 mm to 10 mm in increments of 1 mm. The highest percentage frequency drop for a 10 mm notch radius is around 4.20%, with the obtained 1T frequency being 868.439 Hz.

First Torsional (1T) frequency comparison for various notch radius ranges from 2 mm to 6 mm in increments of 2 mm, with varying notch height locations of 20 mm, 80 mm, 100 mm, 120 mm, and 150 mm from the blade's root to its tip along the leading edge. Graph 2 illustrates that the frequency variation is negligible. Regarding the starting settings, the Second

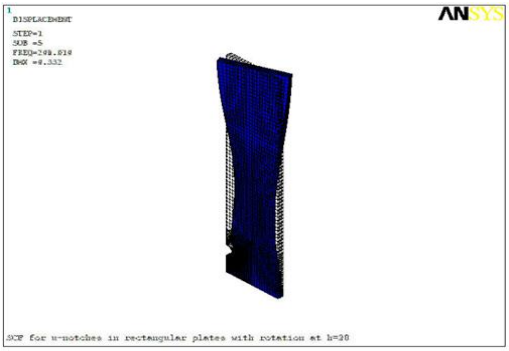

Figure 6: 1T mode of rectangular blade with semicircular notch at h = 20mm

The flexural (2F) frequency is 1201 Hz. The 2F frequency falls as the notch radius is increased in increments of 1 mm from 1 mm to 10 mm while maintaining a constant location height of 20 mm. For a notch radius of 10 mm, the (2F) frequency is 1195 Hz. About 0.499% is the highest percentage drop in 2F frequency. Figure 7 illustrates that the second torsional frequency (2T) of a 1 mm radius notch 20 mm from the blade root is 2783 Hz. The frequency obtained for a 10 mm notch radius is 2698 Hz, when the notch radius is adjusted from 1 mm to 10 mm in increments of 1 mm while maintaining a constant location height of 20 mm from the root.

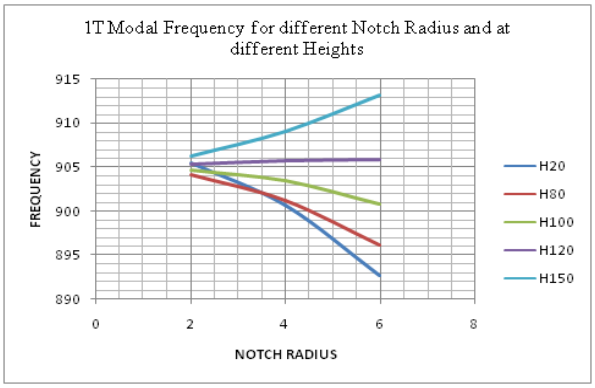

Graph 2: 1t Modal Frequency Vs Notch Radius

ISSN No. 2454-6194 | DOI: 10.51584/IJRIAS |Volume X Issue VI June 2025

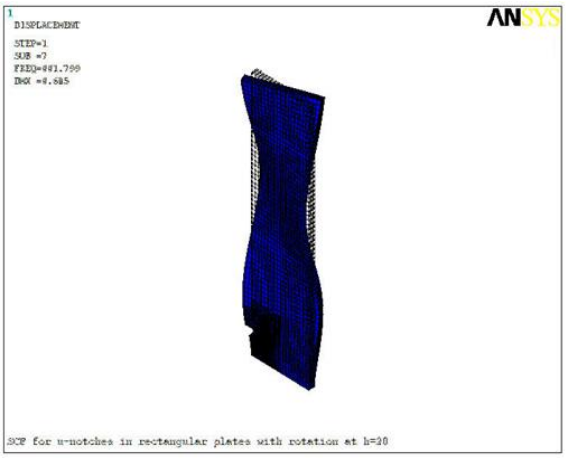

Figure 7: 2T mode of rectangular blade with semicircular notch at h = 20mm

The frequency drops, with a maximum percentage drop of 3.05% in the frequency (2T). Analyzed for different notch heights (50, 80, 100, 120, and 150 mm from the root on the blade's leading edge) and semicircular notch radii ranging from 1 mm to 10 mm in increments of 1 mm, it is found that 1F, 2F, 1T, and 2T frequencies exhibit the same pattern as previously noted. Natural frequencies obtained with the notch at the tip of the beam are marginally higher than those produced with the notch at the root of the beam. The beam's natural frequencies rise at the notch site that is far from the root of the cantilever beam.

CONCLUSION

In order to forecast the modal values, the natural frequency and mode morphologies of a rectangular cantilever beam rotating at a constant speed (15000 rpm) have been investigated for a range of notch parameter possibilities. These parameters are utilized to convert nicks and dents to a notch of known geometry. The impact of notches on cantilever beams—an idealization of blades exposed to FOD—has been attempted to be addressed. The frequency rises when the notch placement shifts from the root to the tip. When the notch diameter increases, the frequency of the rotating cantilever plate rises; conversely, when the location height increases, the frequency falls.

The aerofoil blade's midsection and tip cannot accommodate large notch sizes due to the significant rise in modal frequency. Since the centrifugal field is substantially changed at the blade's root, large notches are not possible, which could negatively impact the aerofoil's overall strength. Since the results of the Finite Element Method accord well with the closed form solution, this methodology can be applied to aerofoils.

REFERENCES

1. Assessment Of Foreign Object Damage (FOD) In Aero Engine Blades. P. Duó[1]*, D. Nowell[1] and J. Schofield[2] Dept. of Eng. Science, University of Oxford, Parks Rd, Oxford, OX1 3PJ, UK. 2Rolls-Royce plc, PO Box 31, Derby, DE24 8BJ. UK
2. Theoretical And Experimental Dynamic Analysis of Fiber Reinforced Composite Beams V. Tita, J. de Carvalho and J. Lirani Dept. of Mechanical Engineering University of S. Paulo 13560-250 S. Carlos, SP. Brazil voltita@sc.usp.br,
3. The Residual Stress State Due To A Spherical Hard-Body Impact B. L. Boyce1, X. Chen2, J. W. Hutchinson2, and R. O. Ritchie1Harvard University, Cambridge, MA 02138, USA
4. Effect of Centrifugal Force On The Elastic Curve Of A Vibrating Cantilever Beam. By Scott H. simpkinson, Laurel .J. Eatherton and Morton. B. Millenson. AERL Clevelend, Ohio.
5. An Investigation Of Fatigue Failures Of Turbine Blades In A Gas Turbine Engine By Mechanical Analysis Jianfu Hou *, Bryon J. Wicks, Ross A. Antoniou Engineering Failure Analysis 9 (2002) 201–211
6. Southwell, R. and Gough, F. The free transverse vibration of airscrew blades Br. A.R.C. Rep. and Memo 1921 (766)

ISSN No. 2454-6194 | DOI: 10.51584/IJRIAS |Volume X Issue VI June 2025

7. Schilhansl, M. Bending frequency of a rotating cantilever beam. Trans. ASME, J. Appl. Mechanics, 1958, 25, 28–30.
8. Leissa A. Vibration Aspects Of Rotating Turbomachinery Blades. Applied Mechanics Reviews (ASME) 1981;34(5):629 –635.
9. Rao J. Turbomachine blade vibration. The Shock And Vibration Digest 1987; 19:3 10.
10. Dokainish M, Rawtani S. Vibration Analysis Of Rotating Cantilever Plates. International Journal for NumericalMethods in Engineering 1971; 3:233–248.
11. Ramamurti V, Kielb R. Natural Frequencies Of Twisted Rotating Plates. Journal of Sound and Vibration 1984; 97(3):429– 449.
12. Flapwise Bending Vibration Of Rotating Plates H. H. Yoo and S. K. Kim Dept. of Mechanical Engineering; Hanyang University; Sungdong-Gu; Haengdang-Dong 17; Seoul; Korea
13. Experimental Modal Analysis of A Turbine Blade M.L.J. Verhees DCT 2004.120